Phosphotyrosine-Containing Dipeptides as High-Affinity Ligands for the p56*lck* SH2 Domain

Montse Llinàs-Brunet,* Pierre L. Beaulieu, Dale R. Cameron, Jean-Marie Ferland, Jean Gauthier, Elise Ghiro, James Gillard, Vida Gorys, Martin Poirier, Jean Rancourt, and Dominik Wernic

Boehringer Ingelheim (Canada) Ltd., Bio-Méga Research Division, 2100 Cunard Street, Laval, Québec H7S 2G5, Canada

Raj Betageri, Mario Cardozo, Scott Jakes, Suzanne Lukas, Usha Patel, John Proudfoot, and Neil Moss

Boehringer Ingelheim Pharmaceuticals Inc., 175 Briar Ridge Road, Ridgefield, Connecticut 06877

Src homology-2 (SH2) domains are noncatalytic motifs containing approximately 100 amino acid residues that are involved in intracellular signal transduction. The phosphotyrosine-containing tetrapeptide Ac-pYEEI binds to the SH2 domain of p56*lck* (Lck) with an affinity of 0.1 μM. Starting from Ac-pYEEI, we have designed potent antagonists of the Lck SH2 domain which are reduced in peptidic character and in which the three carboxyl groups have been eliminated. The two C-terminal amino acids (EI) have been replaced by benzylamine derivatives and the pY + 1 glutamic acid has been substituted with leucine. The best C-terminal fragment identified, (*S*)-1-(4-isopropylphenyl)ethylamine, binds to the Lck SH2 domain better than the C-terminal dipeptide EI. Molecular modeling suggests that the substituents at the 4-position of the phenyl ring occupy the pY + 3 lipophilic pocket in the SH2 domain originally occupied by the isoleucine side chain. This new series of phosphotyrosine-containing dipeptides binds to the Lck SH2 domain with potencies comparable to that of tetrapeptide **1**.
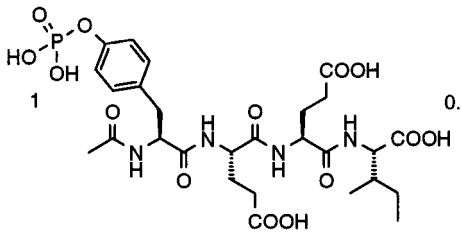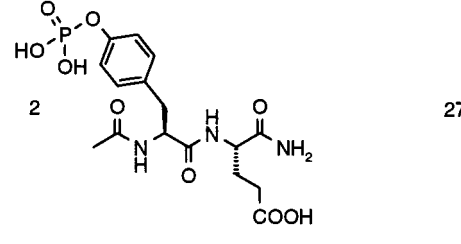
Introduction

A universal feature of intracellular signal transduction and transmission in mammalian cells is the transient association between specific proteins mediated by distinct functional modules such as Src homology-2 (SH2) domains.[1] SH2 domains contain about 100 amino acid residues and are present in many intracellular signal transduction proteins.[2] Their physiological function is to bind phosphotyrosine (pY)-containing peptides which they recognized in the context of immediately adjacent amino acid sequences.[3]

The protein p56*lck* (Lck) is a Src-like lymphocyte-specific tyrosine kinase that plays a key role in the initiation of T cell receptor (TCR) signaling events.[4] Lck is also thought to play a crucial role in T cell development since mice deficient in Lck or expressing a dominant-negative mutant form of Lck exhibit a severe defect in T cell function.[5,6] We believe that selective inhibitors of Lck must be of benefit in the treatment of T cell leukemias and lymphomas and autoimmune diseases such as rheumatoid arthritis.

Like other Src kinases, Lck is made up of five domains: N-terminal, SH3, SH2, kinase, and C-terminal noncatalytic domain.[2] The SH2 domain of Lck is essential for the initiation of signaling events following TCR stimulation, probably by mediating an interaction between Lck and the Zap-70 tyrosine kinase and/or the ζ subunit of the T cell receptor.[7] In addition to a role in interacting with other proteins, the SH2 domain of Src-like kinases also regulates the kinase activity of these enzymes by intramolecularly binding the negative regulatory pY residue located in the C-terminus domain.[8]

A phosphopeptide library screen used to generate a preferred binding sequence for the Lck SH2 domain

Table 1

showed a preference for the sequence Glu-Glu-Ile in the three positions C-terminal to the phosphotyrosine.[9] Crystal structures show that peptides containing the pYEEI motif bind to the Src and Lck SH2 domains in an extended conformation[10,11] and make the most extensive contacts through the phosphotyrosine residue and the isoleucine side chain. The tetrapeptide Ac-pYEEI (compound **1**, Table 1) binds to the Lck SH2 domain with high affinity (K_D = 0.1 μM). However, tetrapeptide **1**, in addition to the phosphate group, contains three carboxylic acid residues that will be negatively charged under physiological conditions. In

order for Lck SH2 domain antagonists to be efficacious in vivo, they have to be able to get inside T cells, and molecules containing multiple anionic groups such as carboxylates are not generally considered good at penetrating the lipophilic cell membrane. A series of di- and tripeptides containing a lipophilic substituent at the C-terminus have been described as antagonists of other SH2 domains of the Src family such as the pp60[src] SH2 domain.[12−17] However, the majority of these dipeptide antagonists still contain the Ac-pYE sequence.[13−16] Two of the studies also describe the replacement of the pY + 1 glutamic acid with a non-carboxylic-acid-containing residue.[12,17] This report concentrates on our efforts to replace the three C-terminal amino acids (EEI) of tetrapeptide **1** with non-carboxyl-containing substitutions while maintaining inhibitory potency.
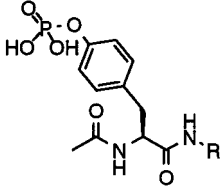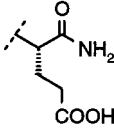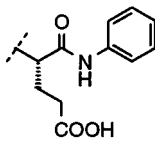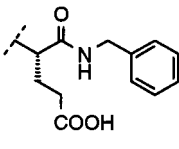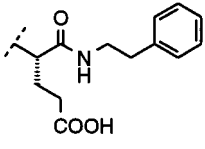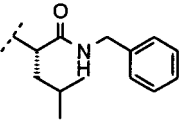
Results and Discussion

The phosphotyrosine-containing tetrapeptide **1** (Table 1) binds with high affinity to the recombinant SH2 domain of Lck ($K_D = 0.1$ μM).[18] A crystal structure of compound **1** bound to the Lck SH2 domain[11] shows the peptide bound in a relatively extended conformation and having the following ligand-protein interactions: there are H-bonds between the protein and the oxygen atom of the Ac-group (pY − 1) and the hydrogen atom of the amide bond between phosphotyrosine (pY) and glutamic acid (pY + 1); the phosphate group is situated in a highly hydrophilic binding pocket and is involved in an intricate network of hydrogen-bonding and charge−charge interactions. The importance of the phosphate group for binding is evidenced by the fact that Ac-YEEI has no measurable binding affinity toward the Lck SH2 domain at concentrations up to 1 mM.[19] One face of the aromatic ring of the pY side chain lies against the aliphatic portion of a Lys side chain. The other face interacts with the guanidinium group of an Arg residue. The remaining significant interaction between compound **1** and the SH2 domain is between the isoleucine side chain and a lipophilic binding pocket in the protein.

Consistent with the X-ray structure of tetrapeptide **1** complexed with the Lck SH2 domain, early structure−activity relationship (SAR) studies indicated that a wide range of amino acid substitutions are independently well-tolerated at both pY + 1 and pY + 2 positions.[18] In particular, leucine, phenylalanine, and glutamine, amino acids with uncharged side chains, are all good replacements for glutamic acid at pY + 1 or pY + 2. Also, the isoleucine at pY + 3 can be replaced by a simple (*S*)-2-methylbutylamine without loss in binding affinity. Leucine-containing tetrapeptides Ac-pYLEI (K_D = 0.1 μM) and Ac-pYELI (K_D = 0.1 μM) display similar binding affinities and a potency comparable to that of compound **1**. However, when two changes are introduced in the same molecule, then a substantial drop in potency results. Simultaneous introduction of Leu at pY + 1 and pY + 2 (Ac-pYLLI) produced a 10-fold drop in binding affinity toward the Lck SH2 domain. These early studies on compound **1** suggested that we were not going to be able to replace all the carboxyl groups and maintain potency by incorporating lipophilic amino acid derivatives.

C-Terminal truncation on compound **1** (Table 1) yielded phosphotyrosine-containing dipeptide **2** (Table
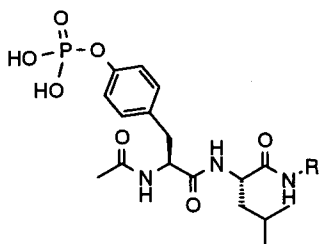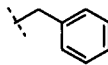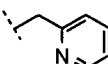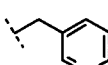
Table 2
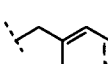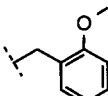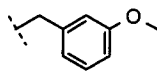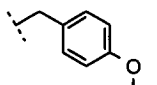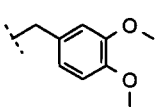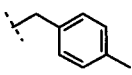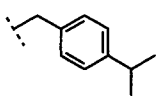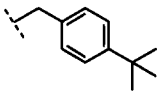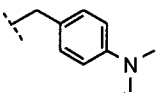
Compound	R	Kd (μM)
2		27
3		8
4		1.5
5		4
6		16

1) with a K_D of 27 μM. Compound **2** was used as a starting point to identify new C-terminal appendages that could reach and occupy the hydrophobic binding pocket originally occupied by the isoleucine side chain. Toward that end, a number of aliphatic and aromatic residues were introduced at the C-terminus of dipeptide **2**.

Table 2 shows the effect of positioning a phenyl ring at the C-terminus of compound **2**. Benzyl derivative **4** attracted our attention because of its simplicity and also because two carboxylic-acid-containing amino acids (EI) could be eliminated despite a 15-fold reduction in potency from tetrapeptide **1**. This study provided us with a new starting point for further SAR. To test the effect of eliminating the remaining carboxylic acid residue, a number of amino acids with lipophilic side chains were introduced at the pY + 1 position. Unfortunately, all the substitutions tried resulted in a substantial loss in potency. The best lipophilic replacement for the pY + 1 glutamic acid residue was leucine (compound **6**) which gave a 10-fold decrease in binding

Table 3

Compound	R	Kd (µM)
6		16
7		31
8		34
9		16
10		17
11		9
12		1.5
13		12
14		2.5
15		0.8
16		8
17		20

affinity compared to **4**. Compound **6** with a K_D of 16 µM, but containing no carboxyl groups, became a new frame of reference for further optimization.

Variation in the Nature of RHS. Initial investigations showed that replacement of the C-terminal phenyl ring in compound **6** by a pyridyl derivative (compounds **7**−**9**, Table 3) had little effect on potency. Likewise, introduction of a methoxy substituent at the 2- or 3-position (compounds **10** and **11,** respectively) of the

phenyl ring had no effect on potency. However, when the methoxy substituent was introduced at the 4-position (compound **12**), a greater than 10-fold increase in binding affinity was observed. Interestingly, the beneficial effect of the 4-methoxy substituent was lost when an additional methoxy group was introduced at the 3-position (compound **13**). Because of the observed increase in potency by the addition of a 4-methoxy substituent on the C-terminal phenyl ring of our ligands, we explored additional substitutions at this position. Compound **14** (Table 3) containing a 4-methyl group had potency similar to that of compound **12**. However, when the size of the alkyl group was increased to an isopropyl group (compound **15**), the potency of the ligand increased by 3-fold. A further increase in the size of the alkyl substituent to a *tert*-butyl group (compound **16**) was detrimental to potency ($K_D = 8$ µM). The interaction of the 4-substituent on the aromatic ring with the SH2 domain appears to be very sensitive to small structural changes as evidenced by the 26-fold loss in potency upon replacement of the 4-isopropyl group in compound **15** by a 4-dimethylamino group (compound **17**, $K_D = 20$ µM).

We have been unsuccessful in obtaining a crystal structure of any of this new series of ligands bound to the Lck SH2 domain. Computational chemistry studies have been performed with this series of analogues, and suitable models for protein−ligand complexes have been derived. In particular, docking and molecular dynamic (MD) refinement have been carried out for compound **12** and the corresponding pY + 1 glutamic acid analogue **18** which, as expected, binds to the Lck SH2 domain with higher affinity ($K_D = 0.2$ µM).

Two low-energy conformations have been derived for compound **12** bound to the SH2 domain of Lck. The only difference between these models is in the bound conformation adopted by the 4-methoxy substituent (Figure 1). In both models, the C-terminal 4-methoxybenzyl group is oriented toward the pY + 3 hydrophobic pocket, with the 4-methoxy substituent located deep in the pocket. Figure 2 highlights the closest contacts of the 4-methoxyphenyl portion of compound **12** with the amino acid residues of the protein. In these models, the aromatic ring is located perpendicular to the plane of Tyr181, in a favorable position for an edge-to-face aromatic−aromatic interaction which may explain the fact that the C-terminal benzyl group was optimal compared to phenyl and phenethyl (Table 2). Moreover, the methyl group of the 4-methoxy substituent is in van der Waals contact with Ile193, Ser194, Leu216, and Gly215. The binding models shown in Figure 2 are consistent with most of the SAR reported in Table 3 and explain the importance of the methoxy substituent at the 4-position of the aromatic ring. Since the two models differ primarily in the positioning of the 4-methoxy substituent, there is evidently enough space to accommodate larger groups consistent with the fact that compound **15**, the 4-isopropyl analogue, has slightly better affinity. The increase in the hydrophobic contacts for the 4-isopropyl group may explain the enhancement of the binding affinity of compound **15**. In addition, a larger substituent such as 4-*tert*-butyl (compound **16**) and disubstitued analogues such as the 3,4-dimethoxy
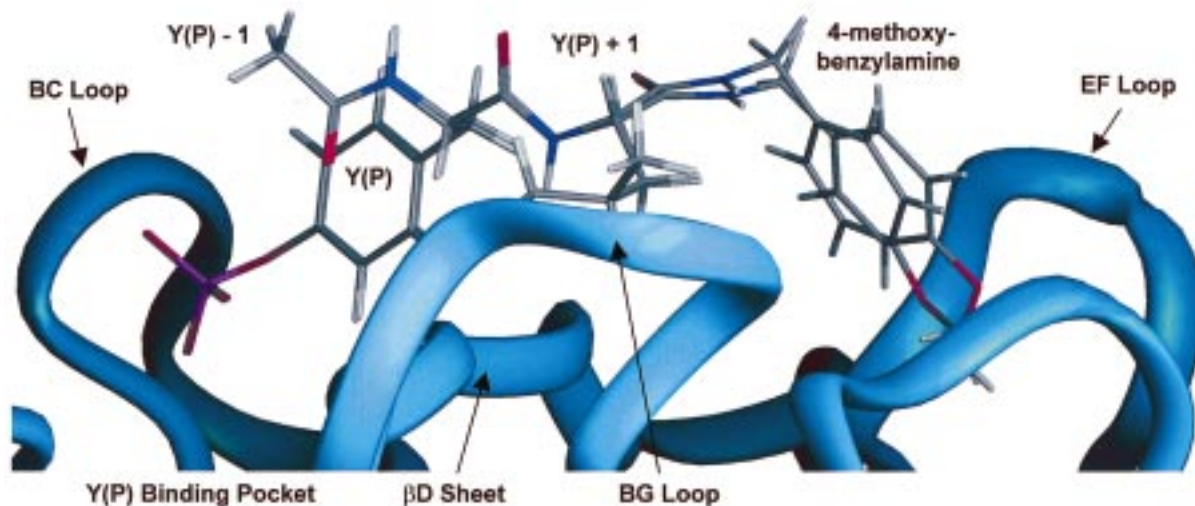
Figure 1. Two models of compound **12** bound to the p56*lck* SH2 domain. The binding pocket of the SH2 domain is highlighted. The pY binding pocket is located between loop BC and sheet βD. The pY + 3 binding pocket is located between loops BG and EF. The protein backbone is highlighted as a blue ribbon with no side chains shown. Two superimposed positions for ligand **12** are shown, and the ligands are colored by atom type as follows: carbon, gray; oxygen, red; nitrogen, dark blue; phosphorus, violet; hydrogen, white.
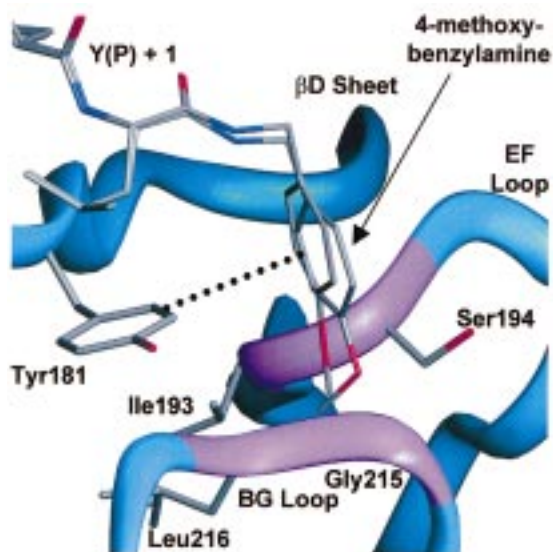
Figure 2. 4-Methoxylbenzylamine binding pocket for two bound models of compound **12**. The protein backbone is depicted as a ribbon and is colored violet where direct contact with ligand **12** is seen. A potential edge–face aromatic interaction is shown as a dotted line. Protein side chains and the ligand **12** are colored as in Figure 1.

analogue **13** appear too bulky to properly bind in the hydrophobic pocket.

Our computational study also provides a rational for the significant difference observed in binding affinity between compounds **12** and the corresponding pY + 1 glutamic acid derivative **18**. Compound **18** is a much better ligand than the corresponding leucine analogue **12**. Molecular dynamic results indicate that the carboxylic group of pY + 1 Glu in compound **18** is able to form hydrogen bonds to Lys179 and Tyr181 (Figure 3). The lack of these hydrogen bonds for pY + 1 Leu may explain the 10-fold difference in binding affinity between these analogues. Interestingly, as mentioned previously for tetrapeptide **1,** this difference in binding affinity between Glu and Leu at pY + 1 position is not observed, and in the crystal structure of the **1**–SH2 complex, as
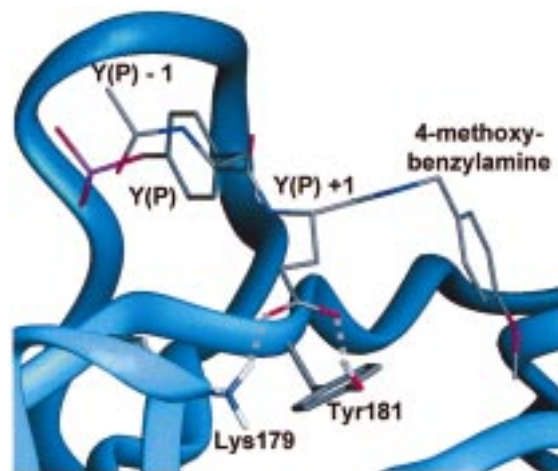
Figure 3. Model of compound **18** bound to the p56*lck* SH2 domain. The protein and compound **18** are colored as in Figure 2. Hydrogen bonds between the pY + 1 carboxylate and protein side chains are shown as dashed lines.
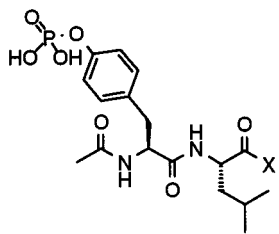
well as in MD simulations, the pY + 1 Glu is not involved in hydrogen bonding with Lys179 or Tyr181.
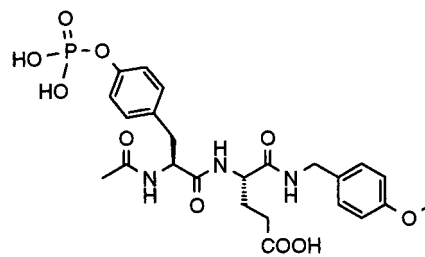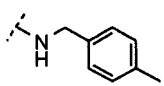
Compound **18** K_d = 0.2 μM

A possible explanation for this difference between the tetrapeptide and dipeptide series is that in the former, the pY + 1 glutamic acid side chain and its carbonyl backbone have some water-mediated interactions with amino acid residues on the side of the protein opposite to Lys179 and Tyr181. This network of polar interac-

Table 4

Compound	X	Kd (µM)
14		2.5
19		2
20		1.5
21		27
22		0.2

tions may prevent the tetrapeptide from moving in the direction of Lys179 and Tyr181, and the pY + 1 Glu is too far from any hydrogen bond donor groups on the protein surface.

These molecular modeling studies also suggested that alkylation of the amido or the adjacent methylene group at the C-terminus of compound **12** should not interfere with binding to the Lck SH2 domain. In addition, these modifications have been reported to increase potency in a similar series of peptidomimetic ligands for the pp60[src] SH2 domain.[17] In our series of ligands, *N*-methylation of the C-terminal amide bond (compound **19**, Table 4) was well-tolerated but did not improve potency over the unsubstituted analogue. A configurationally defined methyl group was also introduced at the α-position of the benzyl amide. Compound **20** having an α-methyl group with the *S*-configuration ($K_D = 1.5$ µM) was slightly more potent than the corresponding unsubstituted analogue (compound **14**, $K_D = 2.5$ µM). On the other hand, compound **21** having the α-methyl group with the *R*-configuration ($K_D = 27$ µM) was 10-

fold less potent than the corresponding unsubstituted analogue. When an (*S*)-α-methyl group was introduced along with a 4-isopropyl group in the C-terminal benzylamine (compound **22**), a 4-fold increase in potency was observed compared to unsubstituted analogue **15** (Table 3). The increase in potency that is gained from α-substitution is dependent on the configuration but is independent of the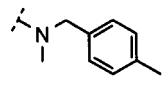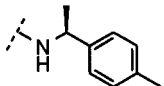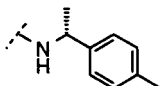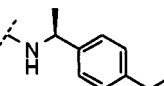 nature or size of the group at the α-position. Indeed, similar results have been obtained with groups such as hydroxymethyl and phenyl with the appropriate configuration (data not shown). With compound **22** ($K_D = 0.2$ µM) we succeeded in eliminating all the carboxyl groups in the molecule while maintaining a potency comparable to that of our original lead tetrapeptide compound **1** ($K_D = 0.1$ µM).

Conclusion

This report reveals a new series of Lck SH2 domain ligands that do not contain any carboxylic acid groups. The starting point in our studies was Ac-pYEEI (compound **1**) which in addition to the phosphotyrosine contains three carboxylic-acid-containing residues. We have demonstrated that the two C-terminal residues in **1** (EI) could be replaced by 4-methoxybenzylamine. Compound **18** containing a single carboxylic acid group and a 4-methoxybenzylamine has a binding affinity toward the Lck SH2 domain almost equivalent to that of tetrapeptide **1**. The last carboxylic-acid-containing residue, pY + 1 Glu, was replaced by leucine with a 10-fold loss in potency. However, potency could be regained by introducing an isopropyl substituent at the 4-position of the C-terminal phenyl ring and a configurationally defined methyl group at the α-position of the benzylamine. Compound **22** containing an (*S*)-1-(4-isopropylphenyl)ethylamine has a binding potency of 0.2 µM and is thus almost equipotent to the initial tetrapeptide **1**. More significantly, the three carboxylic acid residues have been eliminated and the peptidic character of the ligand has been reduced. Studies directed toward finding a metabolically stable and less charged replacement for the phosphate group in this series of ligands will be reported shortly.

Experimental Section

General. NMR spectra were recorded on a Bruker AMX400 (400 MHz for ^{1}H NMR) spectrometer and were referenced to TMS as an internal standard (0 ppm δ scale). Data are reported as follows: chemical shift (ppm), multiplicity (s = singlet, d = doublet, t = triplet, q = quartet, br = broad, m = multiplet), coupling constant (J, reported to the nearest 0.5 Hz), and integration. FAB mass spectra were obtained from a MF 50 TATC instrument operating at 6 kV and 1 mA by using thioglycerol or nitrobenzyl alcohol (NBA) as a matrix support. HPLC homogeneities were measured by using an analytical C18 reversed-phase column and two different eluting systems: method a, 0.06% TFA in water−0.06% TFA in acetonitrile gradient (20−100% acetonitrile over 30 min); method b, 20 mM aqueous Na_2HPO_4 (pH 7.4)−acetonitrile gradient (20−75% acetonitrile over 25 min).

Materials. *N*-Acetyl-L-tyrosine, *N*-Fmoc-L-tyrosine, common amines, and *N*-Boc-L-amino acids were obtained from commercial sources. The synthesis of *N*-Fmoc-L-Tyr(PO₃Bn₂)-OH was done as described in ref 20.

(*S*)-1-(4-Isopropylphenyl)ethylamine Hydrochloride Salt (26).[21] The enantioselective synthesis is outlined in Scheme 1. (*S*)-(−)-4-Isopropyl-2-oxazolidinone (2.7 g, 21 mmol) was dissolved in dry THF (40 mL), and the resultant solution was cooled to −40 °C under an argon atmosphere. *n*-BuLi (1.6 M in hexane, 13 mL, 21 mmol) was added dropwise, and the

Scheme 1
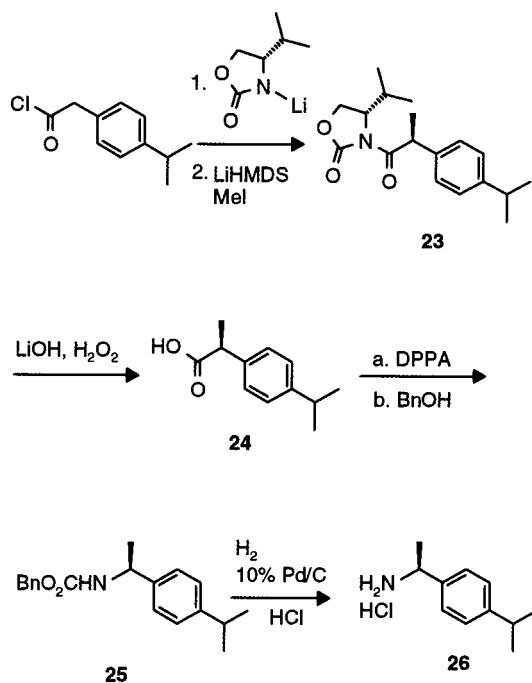
resultant solution was stirred for 30 min at −40 °C. The reaction mixture was cooled to −78 °C, and a solution of (4-isopropylphenyl)acetyl chloride (prepared from the corresponding carboxylic acid and oxalyl chloride under standard conditions) in THF (10 mL) was added dropwise. The mixture was stirred at −78 °C for 30 min and at 0 °C for 1 h. A saturated aqueous solution of NH$_4$Cl (10 mL) was added, and the volatiles were removed under vacuum. The resulting solution was diluted with ethyl acetate (200 mL) and washed with 10% aqueous citric acid (2 × 100 mL), saturated aqueous NaHCO$_3$ (2 × 100 mL), and brine (100 mL). The organic layer was dried (MgSO$_4$), filtered, and concentrated. Flash chromatography of the residue on silica gel eluting with hexanes−ethyl acetate (7:3) gave the desired acyloxazolidinone derivative as a yellow solid (4.9 g, 80% yield): mp 54.5−55.5 °C; [α]^{25}$_D$ +61° (c 1.14, MeOH); ^{1}H NMR (400 MHz, CDCl$_3$) δ 7.23 (d, J = 8 Hz, 2 H), 7.20 (d, J = 8 Hz, 2 H), 4.45 (td, J = 8 and 4 Hz, 1 H), 4.30 (d, J = 15.5 Hz, 1 H), 4.25 (t, J = 8 Hz, 1 H), 4.22 (d, J = 15.5 Hz, 1 H), 4.19 (dd, J = 8 and 3 Hz, 1 H), 2.92−2.85 (m, 1 H), 2.39−2.31 (m, 1 H) 1.23 (d, J = 7 Hz, 6 H), 0.87 (d, J = 7 Hz, 3 H), 0.79 (d, J = 7 Hz, 3 H); HRMS calcd for C$_{17}$H$_{24}$NO$_3$ (MH$^+$) 290.1756, found 290.1741. Anal. Calcd for C$_{17}$H$_{24}$NO$_3$: C, 70.56; H, 8.01; N, 4.84. Found: C, 70.37; H, 8.16; N, 4.89.

A solution of lithium hexamethyldisilazane in THF (1 M, 15.1 mL) was slowly added to a −78 °C solution of the above compound (4.0 g, 13 mmol) in THF (100 mL). After the solution was stirred at −78 °C for 30 min, MeI (0.85 mL, 13 mmol) was added and the mixture was allowed to slowly warm to ambient temperature. After the reaction mixture was stirred for 2 h, 10% aqueous citric acid was added (150 mL). The THF was removed under vacuum, and the aqueous solution was extracted with ethyl acetate (2 × 100 mL). The organic phase was washed with saturated aqueous NaHCO$_3$ (2 × 100 mL) and brine (100 mL), dried (MgSO$_4$), and concentrated. Flash chromatography of the residue on silica gel eluting with hexanes−ethyl acetate (8:2) gave the desired compound **23** as a yellow solid (3.0 g, 71% yield): mp 86−87 °C; [α]^{22}$_D$ +137.5° (c 0.96, MeOH); ^{1}H NMR (400 MHz, CDCl$_3$) δ 7.26 (d, J = 8.5 Hz, 2 H), 7.15 (d, J = 8.5 Hz, 2 H), 5.11 (q, J = 7 Hz, 1 H), 4.37−4.33 (m, 1 H), 4.16−4.13 (m, 2 H), 2.92−2.82 (m, 1 H), 2.47−2.31 (m, 1 H) 1.50 (d, J = 7 Hz, 3 H), 1.22 (d, J = 7 Hz, 6 H), 0.92 (d, J = 7 Hz, 3 H), 0.91 (d, J = 7 Hz, 3 H); HRMS calcd for C$_{18}$H$_{26}$NO$_3$ (MH$^+$) 304.1912, found 304.1899. Anal. Calcd for C$_{18}$H$_{25}$NO$_3$: C, 71.26; H, 8.31; N, 4.26. Found: C, 70.81; H, 8.55; N, 4.56.

Removal of the chiral auxiliary was accomplished by treating a solution of compound **23** (2.6 g, 8.5 mmol) in water (15 mL)−THF (40 mL) with LiOH monohydrate (0.40 g, 10 mmol) and H$_2$O$_2$ (30% aqueous solution, 4.75 mL, 42.2 mmol). After the mixture was stirred at ambient temperature for 3 h, aqueous Na$_2$S$_2$O$_3$ (5.3 g, 37 mmol in 10 mL of water) and saturated aqueous NaHCO$_3$ (5 mL) were added. The THF was removed under vacuum, and the basic aqueous solution was washed with CH$_2$Cl$_2$. The aqueous layer was acidified with 10% aqueous HCl and extracted with ethyl acetate (2 × 50 mL). The organic solution was washed with brine (75 mL), dried (MgSO$_4$), and concentrated to afford the desired acid **24** as a white solid (1.6 g, quantitative yield): mp 55−56 °C; [α]^{22}$_D$ +65.3° (c 1.35, MeOH); ^{1}H NMR (400 MHz, CDCl$_3$) δ 7.24 (d, J = 8 Hz, 2 H), 7.18 (d, J = 8 Hz, 2 H), 3.71 (q, J = 7 Hz, 1 H), 2.94−2.82 (m, 1 H), 1.50 (d, J = 7 Hz, 3 H), 1.23 (d, J = 7 Hz, 6 H); HRMS calcd for C$_{12}$H$_{17}$O$_2$ (MH$^+$) 193.1222, found 193.1228. Anal. Calcd for C$_{12}$H$_{16}$O$_2$: C, 74.97; H, 8.39. Found: C, 74.88; H, 8.78.

The conversion of carboxylic acid **24** to amine **26** was achieved via a Curtius rearrangement:[22] a solution of acid **24** (0.24 g, 1.2 mmol), diphenylphosphorylazide (DPPA) (0.29 mL, 1.3 mmol), and Et$_3$N (0.19 mL, 1.4 mmol) in THF (5 mL) was heated at reflux for 2 h. Benzyl alcohol (0.38 mL, 3.7 mmol) was added, and the mixture was heated to reflux for an additional 16 h. The reaction mixture was allowed to cool to ambient temperature, and ethyl acetate (100 mL) was added. The organic solution was washed with 10% aqueous citric acid (2 × 50 mL), saturated aqueous NaHCO$_3$ (2 × 50 mL), and brine (50 mL), dried (MgSO$_4$), filtered, and concentrated. Flash chromatography of the residue on silica gel eluting with hexanes−ethyl acetate (8:2) gave carbamate **25** as a white solid (0.22 g, 60% yield): mp 95−96 °C; [α]^{22}$_D$ −52.6° (c 1.12, MeOH); ^{1}H NMR (400 MHz, CDCl$_3$) δ 7.35−7.25 (m, 4 H), 7.23−7.17 (m, 5 H), 5.11 (d, J = 12 Hz, 1 H), 5.06 (d, J = 12 Hz, 1 H), 4.82−4.88 (m, 1 H), 2.93−2.86 (m, 1 H), 1.48 (d, J = 6.5 Hz, 3 H), 1.24 (d, J = 7 Hz, 6 H); HRMS calcd for C$_{19}$H$_{24}$NO$_2$ (MH$^+$) 298.1807, found 298.1790. Anal. Calcd for C$_{19}$H$_{23}$NO$_2$: C, 76.73; H, 7.79; N, 4.71. Found: C, 76.52; H, 8.02; N, 4.90.

To a solution of benzyl carbamate **25** (1.09 g, 3.7 mmol) in EtOH (20 mL) was added 10% Pd/C (100 mg), and the mixture was stirred under 1 atm of H$_2$ for 45 min. The catalyst was removed by filtration through a Millex HV 0.45-μm filter, and to the clear solution was added 1 N HCl solution in ether (7.3 mL). The mixture was concentrated to yield the desired amine hydrochloride salt **26** as an off-white solid (0.68 g, 82% yield): mp 180 °C dec; [α]^{22}$_D$ −7.5° (c 2.20, MeOH); ^{1}H NMR (400 MHz, CDCl$_3$) δ 8.67 (br s, 3 H), 7.39 (d, J = 8 Hz, 2 H), 7.21 (d, J = 8 Hz, 2 H), 4.40−4.25 (m, 1 H), 2.91−2.84 (m, 1 H), 1.63 (d, J = 7 Hz, 3 H), 1.22 (d, J = 7 Hz, 6 H); HRMS calcd for C$_{11}$H$_{18}$N (MH$^+$) 164.1439, found 164.1448.

***N*-Acetyl-L-Tyr(PO$_3$Bn$_2$)-OH (27).** To a solution of *N*-acetyl-L-tyrosine (5.0 g, 22 mmol) in THF (150 mL) were added *tert*-butyldimethylsilyl chloride (3.4 g, 22 mmol) and *N*-methylmorpholine (2.5 mL, 22 mmol). After 5 min, *1 H*-tetrazole (6.3 g, 90 mmol) and dibenzyldiisopropylamine phosphoramidite (11.3 mL, 33 mmol) were added, and the solution was stirred for an additional 3 h. The reaction mixture was cooled to 0 °C, and 14% aqueous *tert*-butyl hydroperoxide (16.0 mL, 51 mmol) was added. After 30 min at 0 °C and 1 h at ambient temperature, the solution was cooled again to 0 °C, and 10% aqueous sodium thiosulfate (200 mL) was added. The solution was rapidly stirred for 1 h at ambient temperature followed by removal of THF under reduced pressure and addition of ether−ethyl acetate (1:1, 500 mL). The organic solution was extracted with saturated aqueous NaHCO$_3$ (2 × 250 mL). The aqueous layer was acidified with 6 N HCl and extracted with ethyl acetate (2 × 200 mL). The organic solution was washed with brine, dried (MgSO$_4$), and concentrated to give the desired compound **27** as a colorless foam (9.2 g, 85% yield): [α]^{25}$_D$ +74° (c 1.37, CHCl$_3$); ^{1}H NMR (400 MHz, DMSO-d$_6$) δ 8.17 (d, J = 8 Hz, 1 H), 7.40−7.32 (m, 10 H), 7.22 (d, J = 8.5 Hz, 2 H), 7.09 (d, J = 8.5 Hz, 2 H), 5.15 (s, 2 H) 5.13 (s, 2 H), 4.41−4.36 (m, 1 H), 3.02 (dd, J = 14, 5 Hz, 1 H), 2.82

(dd, *J* = 14, 10 Hz, 1 H), 1.78 (s, 3 H); HRMS calcd for $C_{25}H_{27}$-NO_7P (MH$^+$) 484.1525, found 484.1538.

Inhibitor Synthesis. 1. Synthesis of Inhibitors in Tables 1 and 2 (except Compound 6) and Compound 18. All these inhibitors were prepared by sequentially coupling simple amines, *N*-Boc-amino acid derivatives, or *N*-Fmoc-Tyr-(PO$_3$Bn)-OH from C− to N-terminus by using benzotriazol-1-yl-1,1,3,3-tetramethyluronium tetrafluoroborate (TBTU) as the coupling agent. Removal of the *N*-Boc protective group was effected with 4 N HCl in dioxane. The *N*-Fmoc protective group was removed by treatment with DBU in DMF. The following procedure is representative.

To a solution of *N*-Boc-amino acid or *N*-Fmoc-Tyr(PO$_3$Bn)-OH (1 mmol) in dry acetonitrile (2.5 mL) were added TBTU (1 mmol) and *N*-methylmorpholine (1 mmol). After ca. 5 min, this solution was added to a solution of amino ester hydrochloride salt, peptide hydrochloride salt, or C-terminal amine (1 mmol) in dry acetonitrile (2.5 mL) containing *N*-methylmorpholine (2 mmol for the hydrochloride salts or 1 mmol for free amines). The reaction mixture was stirred at ambient temperature for 2−6 h (reaction monitored by TLC) and then poured into a mixture of EtOAc (50 mL) and saturated aqueous NaHCO$_3$ (50 mL). The organic phase was further washed with saturated aqueous NaHCO$_3$ (50 mL), 1 N aqueous HCl (2 × 50 mL), and brine (50 mL). Drying (MgSO$_4$), filtration, and concentration provided the peptide, usually of sufficient purity to continue to the next step without further purification. *N*-Boc or *N*-Fmoc derivatives could be purified if necessary by conventional flash chromatography. The *N*-Boc-peptide product (1 mmol) was then treated with 4 N HCl in dioxane (5 mL) for 45 min. The solvent was removed under vacuum, and the resulting hydrochloride salt was subjected to high vacuum before use in the next coupling reaction. The *N*-Fmoc-peptide product was treated with DBU (1.2 mmol) in DMF (5 mL) for 15 min. Saturated aqueous NaHCO$_3$ (4 mL) and ethyl acetate (10 mL) were added. The organic phase was dried (MgSO$_4$), filtered, and concentrated under vacuum, and the resulting amine was used in the next coupling reaction without further purification.

Subsequently, the protected peptide derivatives were purified by flash chromatography, and the benzyl-protecting groups of the phosphotyrosine residue and other acid residues were removed by catalytic hydrogenolysis using 10% P/C (10 wt %) in ethanol and 1 atm of H$_2$ for 2−3 h (reaction monitored by HPLC). The resultant product was usually obtained in greater than 95% purity (HPLC and NMR), but if necessary it was purified by preparative HPLC on a C-18 reversed-phase column (Vydac, 15-μm particle size) eluting with 0.06% aqueous TFA−0.06% TFA in acetonitrile gradients.

2. Synthesis of Inhibitors in Tables 3 and 4. These inhibitors were prepared by solution coupling of the corresponding C-terminal amine to a preformed dipeptide fragment as outlined in Scheme 2. The acetylated dipeptide was synthesized as follows: to a solution of Ac-Tyr(PO$_3$Bn$_2$)-OH (**27**) (4.65 g, 9.6 mmol) in THF (30 mL) were added 1-hydroxybenzotriazole·H$_2$O (1.49 g, 11.1 mmol) and 1,3-dicyclohexylcarbodiimide (2.18 g, 10.6 mmol), and the mixture was stirred at ambient temperature for 30 min. A suspension of leucine allyl ester hydrochloride salt (**28**) and *N*-methylmorpholine (1.1 mL, 9.3 mmol) in THF (30 mL) were added to the above mixture. After stirring at ambient temperature for 4 h, the mixture was filtered, the filtrate concentrated, and the residue dissolved in ethyl acetate (75 mL). The organic solution was washed with 10% aqueous citric acid (2 × 50 mL), saturated aqueous NaHCO$_3$ (2 × 50 mL), and brine (50 mL), dried (MgSO$_4$), and concentrated. Flash chromatography of the residue on silica gel eluting with a gradient from hexanes−ethyl acetate (7:3) containing 1% MeOH to ethyl acetate−1% MeOH gave the desired dipeptide **29** as a colorless gum (4.94 g, 80% yield): ^{1}H NMR (400 MHz, CDCl$_3$) δ 7.38−7.30 (m, 10 H), 7.14 (d, *J* = 8.5 Hz, 2 H), 7.07 (d, *J* = 8.5 Hz, 2 H), 6.23 (d, *J* = 8 Hz, 1 H), 6.10 (d, *J* = 7.5 Hz, 1 H), 5.95−5.85 (m, 1 H), 5.31 (br d, *J* = 17.5 Hz, 1 H), 5.25 (br d, *J* = 10.5 Hz, 1 H), 5.12 (s, 2 H), 5.10 (s, 2 H), 4.66−4.51 (m, 4 H), 3.08−2.98 (m,

Scheme 2
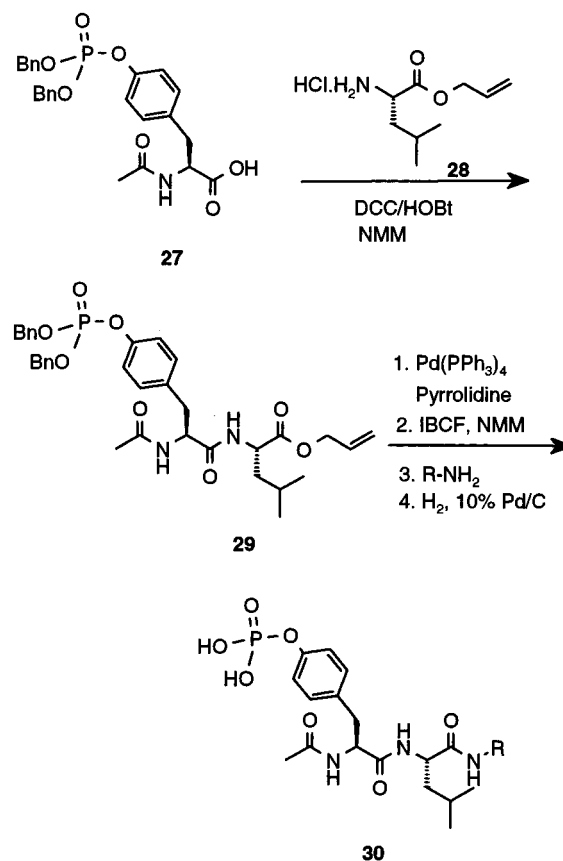
2 H), 1.96 (s, 3 H), 1.68−1.47 (m, 3 H), 0.90 (d, *J* = 6 Hz, 6 H); HRMS calcd for $C_{34}H_{42}N_2O_8P$ (MH$^+$) 637.2679, found 637.2693.

At 0 °C, to a solution of palladium tetrakis(triphenylphosphine) (Pd(PPh$_3$)$_4$) (0.18 g, 0.15 mmol) in acetonitrile−methylene chloride (1:1, 5 mL) was added pyrrolidine (0.78 mL), and the solution was stirred for 5 min. A suspension of allyl ester **29** in acetonitrile−methylene chloride (1:1, 35 mL) was slowly added to the above solution. After stirring the mixture at ambient temperature for 3 h, the volatiles were removed under vacuum. The residue was dissolved in saturated aqueous NaHCO$_3$ (60 mL), and the basic solution was washed with Et$_2$O (2 × 50 mL) and then acidified with 10% aqueous HCl. The acidic solution was extracted with ethyl acetate (2 × 75 mL). The organic layer was washed with brine (100 mL), dried (MgSO$_4$), and concentrated to give the desired carboxylic acid as an off-white solid: mp 130−138 °C dec; ^{1}H NMR (400 MHz, CDCl$_3$) δ 7.38 (br s, 10 H), 7.14 (d, *J* = 8 Hz, 2 H), 6.97 (d, *J* = 8 Hz, 2 H), 6.56 (d, *J* = 8 Hz, 1 H), 5.68 (d, *J* = 9 Hz, 1 H), 5.25−5.14 (m, 4 H), 4.54−4.49 (m, 1 H), 4.42−4.38 (m, 1 H), 3.18 (dd, *J* = 13 and 5.5 Hz, 1 H), 2.72 (t, *J* = 11.5 Hz, 1 H), 4.66−4.51 (m, 4 H), 2.03 (s, 3 H), 1.59−1.52 (m, 1 H), 1.48−1.33 (m, 2 H), 0.89 (d, *J* = 6.5 Hz, 3 H), 0.88 (d, *J* = 6.5 Hz, 3 H); HRMS calcd for $C_{31}H_{38}N_2O_8P$ (MH$^+$) 597.2382, found 597.2382.

The following procedure is representative for the synthesis of the C-terminal amides: At −30 °C, to a solution of the above carboxylic acid (0.15 mmol) in THF (3 mL) were added *N*-methylmorpholine (0.30 mmol) and isobutyl chloroformate (0.18 mmol). The solution was stirred at −30 °C for 30 min, the corresponding C-terminal amine was added (0.15 mmol), and the stirring was continued for an additional hour. A 10% aqueous solution of citric acid (5 mL) was added, and the mixture was warmed to ambient temperature. The mixture was diluted with EtOAc (30 mL) and washed with 10% aqueous citric acid (2 × 20 mL), saturated aqueous NaHCO$_3$ (2 × 20 mL), and brine (20 mL). The organic solution was dried (MgSO$_4$) and concentrated. The protected peptide was purified by flash. Removal of benzyl-protecting groups and purification

of final compounds were carried out as described in the previous example.

3. Inhibitor Characterization and Purity. All peptide derivatives showed satisfactory 400 MHz ^{1}H NMR spectra, FAB mass spectra (M$^+$ + H) and/or (M$^+$ + Na), amino acid analyses including peptide recovery, and HPLC purity in two solvent systems (>95%).

Molecular Modeling. Compounds **12** and **18** were modeled using the crystal structure of the SH2 Lck Ac-Tyr(P)-Glu-Glu-Ile complex[11] as starting geometry. The corresponding pY + 1 residue and the 4-methoxybenzyl substituents were initially positioned in the protein surface using manual docking procedures with the hydrophobic C-terminus located in a similar spatial position as the pY + 3 Ile side chain. Subsequently, a quenching molecular dynamics (QMD) protocol was used to explore alternative docking orientations. The QMD was performed using the program CharmM[23] with a production run of 100 ps and a temperature of 600 K. Following the QMD, a sampling of the molecular dynamics trajectory was performed at every picosecond, and each configuration was energy-minimized using conjugate gradients protocol. The electrostatic Coulombic potential was computed using a distance-dependent dielectric constant of 4 with CharmM charges for the protein and MNDO ESP charges for the ligand, using MOPAC.[24] After energy minimization, a cluster analysis of the ligand atoms was carried out in coordinate space, and the lowest intermolecular energy minimum, for each cluster, was selected as representative of the cluster. Analysis of the structure for the final complex of each cluster obtained identified two suitable protein–inhibitor models for compound **12**. These models were further optimized by performing 400 ps of MD with explicit solvent representation, using a TIP3P[25] solvent cap of 25 Å around the inhibitor. In this MD protocol, all atoms within 13 Å radius around the inhibitor were allowed to move freely. The rest of the protein was tethered as follows: (1) the protein was constrained using a potential harmonic constraint of 5 kcal (Å^2)$^{-1}$; (2) the remaining solvent molecules were maintained within the sphere limit by applying the CharmM DROP restraint option.

Lck SH2 Domain Binding Assay. The binding affinities of these ligands for the Lck SH2 domain were measured in a competitive binding assay. The protein used is a glutathione-*S*-transferase (GST) fusion protein, and the binding constant is determined using surface plasmon resonance according to a published protocol.[15] The reported K_D values are the mean of at least four separate determinations with a standard deviation of ±20%.

Supporting Information Available: Full tabulation of ^{1}H NMR, FAB mass spectra, amino acid analyses, and HPLC purity data for new inhibitors. This material is available free of charge via the Internet at http://pubs.acs.org.

References

(1) Beattie, J. SH2 Domain Protein Interaction and Possibilities for Pharmacological Intervention. *Cell. Signal* **1996**, *8*, 75–86.

(2) Koch, C. A.; Anderson, D.; Moran, M. F.; Ellis, C.; Pawson, T. SH2 and SH3 Domains: Elements that Control Interactions of Cytoplasmic Signaling Proteins. *Science* **1991**, *252*, 668–674.

(3) Songyang, Z.; Shoelson, S. E.; Chaudhuri, M.; Gish, G.; Pawson, T.; Haser, W. G.; King, F.; Roberts, T.; Ratnofsky, S.; Lechleider, R. J.; Neel, B. G.; Birge, R. B.; Fajardo, J. E.; Chou, M. M.; Hidesaburo, H.; Schaffhausen, B.; Cantley, L. C. SH2 Domains Recognize Specific Phosphopeptide Sequences. *Cell* **1993**, *72*, 767–778.

(4) Weil, R.; Veillette, A. Signal Transduction by the Lymphocyte-Specific Tyrosine Protein Kinase p56^{lck}. *Curr. Top. Microbiol. Inmunol.* **1996**, *205*, 63–87.

(5) Molina, T. J.; Kishihara, K.; Siderovski, D. P.; van Ewijk, W.; Narendran, A.; Timms, E.; Wakeham, A.; Paige, C. J.; Hartman, K.-U.; Veillette, A.; Davison, D.; Mark, T. W. A Dominant-Negative Transgene Defines a Role for p56^{lck} in Thymopoiesis. *Nature* **1992**, *357*, 161–164.

(6) Levin, D. S.; Anderson, S. J.; Forbush, K. A.; Perlmutter, R. M. Profound Block in Thymocyte Development in Mice Lacking p56^{lck}. *EMBO J.* **1993**, *12*, 1671–1680.

(7) Strauss, D. B.; Chan, A. C.; Patai, B.; Weiss, A. SH2 Domain Function Is Essential for the Role of the Lck Tyrosine Kinase in T Cell Receptor Signal Transduction. *J. Biol. Chem.* **1996**, *271*, 9976–9981.

(8) Couture, C.; Songyang, Z.; Jascur, T.; Williams, S.; Tailor, P.; Cantley, L. C.; Mustelin, T. Regulation of the Lck SH2 Domain by Tyrosine Phosphorylation. *J. Biol. Chem.* **1996**, *271*, 24880–24884.

(9) Eck, M. J.; Shoelson, S. E.; Harrison, S. C. Recognition of a High-Affinity Phosphotyrosyl Peptide by the Src Homology-2 Domain of p56^{lck}. *Nature* **1993**, *362*, 87–91.

(10) Eck, M. J.; Atwell, S. K.; Shoelson, S. E.; Harrison, S. C. Crystal Structure of the Regulatory Domains of the Src Family Tyrosine Kinase P56^{lck}. *Nature (London)* **1994**, *368*, 764–769.

(11) Tong, L.; Warren, T. C.; King, J.; Betageri, R.; Rose, J.; Jakes, S. Crystal Structures of the Human p56^{lck} SH2 Domain in Complex with Two Short Phosphotyrosyl Peptides at 1.0 and 1.8 Å Resolution. *J. Mol. Biol.* **1996**, *256*, 601–610.

(12) Pacofsky, G. J.; Lackey, K.; Alligood, K. J.; Berman, J.; Charifson, P. S.; Crosby, R. M.; Dorsey, G. F. Jr.; Feldman P. L.; Gilmer, T. M.; Hummel, C. W.; Jordan, S. R.; Mohr, C.; Shewchuk, L. M.; Sternbach, D. D.; Rodriguez, M. Potent Dipeptide Inhibitors of the pp60^{c−src} SH2 Domain. *J. Med. Chem.* **1998**, *41*, 1894–1908.

(13) Plummer, M. S.; Lunney, E. A.; Para, K. S.; Vara Prasad, J. V. N.; Shahripour, A.; Singh, J.; Stankovic, C. J.; Humblet, C.; Fergus, J. H.; Marks, J. S.; Sawyer, T. K. Hydrophobic D-Amino Acids in the Design of Peptide Ligands for the pp60^{Src} SH2 Domain. *Drug Des. Discovery* **1996**, *13*, 75–81.

(14) Plummer, M. S.; Holland, D. R.; Shahripour, A.; Lunney, E. A.; Fergus, J. H.; Marks, J. S.; McConnell, P.; Mueller, W. T.; Sawyer, T. K. Design, Synthesis, and Cocrystal Structure of a Nonpeptide Src SH2 Domain Ligand. *J. Med. Chem.* **1997**, *40*, 3719–3725.

(15) Shahripour, A.; Para, K. S.; Plummer, M. S.; Lunney, E. A.; Holland, D. R.; Rubin, J. R.; Humblet, C.; Fergus, J. H.; Marks, J. S.; Saltiel, A. R.; Sawyer, T. K. Structure-Based Design of Novel, Dipeptide Ligands Targeting the pp60^{src} SH2 Domain. *Bioorg. Med. Chem. Lett.* **1997**, *7*, 1107–1112.

(16) Rodriguez, M.; Crosby, R.; Alligood, K.; Gilmer, T.; Berman, J. Tripeptides as Selective Inhibitors of Src-SH2 Phosphoprotein Interactions. *Lett. Pept. Sci.* **1995**, *2*, 1–6 and references therein.

(17) Plummer, M. S.; Lunney, E. A.; Para, K. S.; Shahripour, A.; Stankovic, C. J.; Humblet, C.; Fergus, J. H.; Marks, J. S.; Herrera, R.; Hubbell, S.; Saltiel, A.; Sawyer, T. K. Design of Peptidomimetic Ligands for the pp60^{src} SH2 Domain. *Bioorg. Med. Chem.* **1997**, *7*, 41–47.

(18) Morelock, M. M.; Ingraham, R. H.; Betageri, R.; Jakes, S. Determination of Receptor–Ligand Kinetics and Equilibrium Binding Constants Using Surface Plasmon Resonance: Application to the *Lck* SH2 Domain and Phosphotyrosyl Peptides. *J. Med. Chem.* **1995**, *38*, 1309–1318.

(19) Unpublished results.

(20) Perich, J. W.; Reynolds, E. C. The Facile One-Pot Synthesis of N^α-(9-Fluorenylmethoxycarbonyl)-O-(O′,O"-Dialkylphosphoro)-L-Tyrosines Using Dialkyl N,N-Diethylphophoramidites. *Synlett* **1991**, 577–578.

(21) Saigo, K.; Kai, M.; Yonezawa, N.; Hasegawa, M. Synthesis and Optical Resolution of 1-(4-Isopropylphenyl)-Ethylamine. *Synthesis* **1985**, *2*, 214–216.

(22) Capson, T. L.; Poulter, C. D. A Facile Synthesis of Primary Amines from Carboxylic Acids by the Curtius Rearrangement. *Tettrahedron Lett.* **1984**, 3515–3518.

(23) Molecular Simulations Inc., Scranton Rd, San Diego, CA 92121-3752.

(24) Steward, J. J. P. *MOPAC Manual*, MOPAC 6.0; Frank J. Seiler Research Laboratory, United State Air Force Academy, 1990.

(25) Jorgensen, W. L.; Briggs, J. M.; Contreras, M. L. *J. Phys. Chem.* **1990**, *94*, 1683–1687.